Effects of organic ligands on Pb absorption and speciation changes in *Arabidopsis* as determined by micro X-ray fluorescence and X-ray absorption near-edge structure analysis

Ya Ting Shen* and Yu Fang Song

National Research Center of Geoanalysis, 26# Xicheng District, Beijing 100037, People's Republic of China. *Correspondence e-mail: shenyating@cags.ac.cn
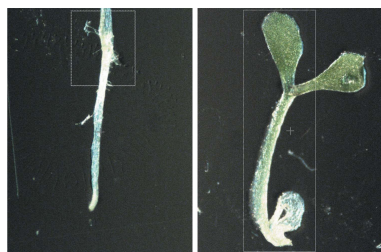
Pb can pass through the food chain *via* plants and threaten human health, which has attracted widespread attention. Changes in Pb speciation affect its bioavailability in soils and water. However, whether organic ligands can change the uptake and mobility of Pb in plants and increase or decrease Pb bioavailability remains uncertain. To reveal the roles of organic and inorganic Pb in Pb metabolism in plants, the localization and speciation changes of Pb in *Arabidopsis thaliana* plants grown in organic and inorganic Pb were characterized by synchrotron radiation micro X-ray fluorescence and X-ray absorption near-edge structure, respectively. These results demonstrated that *Arabidopsis* absorbed more Pb from $Pb(NO_3)_2$ than $Pb(CH_3COO)_2$ at the same exposure concentration. A higher percentage of Pb-citrate was found in *Arabidopsis* exposed to inorganic Pb solution, which suggested that Pb-citrate was the main complex for root-to-shoot transportation in *Arabidopsis* exposed to inorganic Pb solutions. Pb complexed with the organic ligand CH_3COO^- significantly inhibited primary root growth and lateral root development, while, at the same time, Pb was blocked by root hairs, which represented another way to reduce Pb absorption and protect the plant from biotoxicity.

1. Introduction

The heavy metal Pb, which has no essential role in the metabolism of living organisms, is highly pervasive, persistent and toxic (Schreck *et al.*, 2012; Giaccio *et al.*, 2012). Environmental heavy metal contamination is a widespread problem because of the effects of these metals on the environment, plants and human health (Bech *et al.*, 2011; Shahid *et al.*, 2013; Liu & Luo, 2015).

Pb has been reported to inhibit seed germination, root development and cell division (Pourrut *et al.*, 2011). Additionally, Pb promotes active oxygen generation at the cellular level (Wahsha *et al.*, 2012). Understanding Pb detoxification mechanisms in plants is highly important for phytotoxicity risk assessment and phytoremediation studies (Arshad *et al.*, 2008; Schreck *et al.*, 2012).

The total concentrations of heavy metals are not well related to their bioavailability and biotoxicity, and the elemental species need to be considered when studying the effects of heavy metals (Shahid *et al.*, 2011). Most of Pb exists in non-residual fraction, mainly in reducible fraction (Fleming *et al.*, 2013; Wang *et al.*, 2016; Margui *et al.*, 2004; Templeton *et al.*, 2001). However, there are limited data about the effects of species changes on heavy metal absorption, storage and transportation in plants. Thus, it is important to evaluate the

physiological responses of plants to variations in Pb species in the nutrient medium.

Organic ligands are known to affect Pb cycling in terrestrial ecosystems because of their effects on Pb complexation. Organic ligands can change metal speciation and, in turn, metal uptake and toxicity (Kim, Lim *et al.*, 2010; Shahid *et al.*, 2012). It was proposed that metal speciation must be given due consideration in risk assessment and remediation studies (Shahid *et al.*, 2014). However, its role as a mediating factor in plant bioavailability remains uncertain (Orsetti *et al.*, 2013). Organic ligands can significantly increase Pb uptake and mobility, which increase bioavailability, but sometimes reduce the biological effects of Pb by increasing soil adsorption (Babich & Stotzky, 1979). In fact, organo-metallic complexes are quite different from free metal ions in terms of solubility, stability, bioavailability and chronic toxicity (Shahid *et al.*, 2012; Evangelou *et al.*, 2007). Therefore, this study was conducted to compare the effects of inorganic and organic Pb on the absorption, distribution and speciation of Pb in plants.

To reveal the roles of inorganic and organic Pb in Pb metabolism in plants, the model plant *Arabidopsis thaliana* was used in this research. In this study, the Pb distribution in plants and the effects of inorganic and organic Pb were characterized. Root iron plaques and the Pb distribution under organic and inorganic Pb were examined to determine how inorganic and organic Pb affect Pb absorption by the plant. Synchrotron radiation micro X-ray fluorescence (μ-XRF) was used to investigate the distribution and competition distribution characteristics of Pb in *Arabidopsis* plants, while X-ray absorption near-edge structure (XANES) was used to examine Pb speciation. Using experimental data for plants grown in nutrient solutions with organic or inorganic Pb, Pb accumulation and speciation, root length, lateral root density, root Fe and Pb distributions and long-distance Pb transportation in *Arabidopsis* were investigated.

2. Experimental

2.1. Plant sample preparation

Seeds of *A. thaliana* ecotype Columbia were surface sterilized with 0.2% Triton-100 and 10% NaClO for 12 min, washed with sterilized distilled water three times and sown in nutrient solution. Then, the seeds were incubated in the dark for 3 days at 4°C to synchronize germination. The composition of the modified nutrient solution was as follows: 475 mg KNO_3, 82.5 mg $CaCl_2$, 45 mg $MgSO_4$, 42.5 mg NH_4NO_3 and 312 mg KH_2PO_4. The plants were grown under natural light, at a temperature of around 26°C and a humidity of 30%. After seedling emergence, the Pb concentration in the culture solution was raised gradually to a set value using 10 mM $Pb(NO_3)_2$ over the following three days to avoid acute poisoning. Nutrient solutions with $Pb(NO_3)_2$ or $Pb(CH_3COO)_2$ were prepared with different concentration gradients between 0 and 200 p.p.m. Three repeat samples and three blank controls were used.

2.2. Standard reference preparation

Powders and tablets of standard materials of $Pb(C_{17}H_{35}COO)_2$, $C_{32}H_{66}PbS_2$, Pb-PbO, Pb_3O_4, $Pb(CH_3COO)_2$, PbS, $PbCO_3Pb(OH)_2$, $PbSO_4$, $Pb(NO_3)_2$, $PbCl_2$, $PbCO_3$, $Pb(OH)_2$, $Pb_5Cl(PO_4)_3$ and $Pb_3(PO_4)_2$ for μ-XRF and μ-XANES were prepared previously. A liquid standard of Pb-citric acid was mixed from 0.1 mol L^{-1} citric acid and 0.05 mol L^{-1} $Pb(NO_3)_2$. A liquid standard of Pb-fulvic acid (Pb-FA) was mixed from 0.05 mol L^{-1} $Pb(NO_3)$ and 13.35 mg FA (Suwannee River I), which was purchased from the International Humic Substances Society (St Paul, MN, USA).

2.3. Total Pb content analysis

After the Columbia *Arabidopsis* was cultured for one month, samples were collected and washed with deionized water, frozen and dried for 12 h, ground into a uniform powder in liquid nitrogen, and dried in an oven at 40°C to a constant weight. Pre-digestion was performed in a polytetrafluoroethylene digestion tank with 1 ml 30% H_2O_2 and 5 ml 70% HNO_3, and then 2 ml 30% H_2O_2 and 5 ml 70% HNO_3 were added for closed-vessel digestion. Elemental contents were measured using ICP-MS (NexION 300Q, PerkinElmer). Each sample was analyzed by ICP-MS at least three times. Three biological standard materials, GSB-6, GSB-7 and GSB-11, were used for quality monitoring.

2.4. Synchrotron radiation μ-XRF acquisition

Plants were taken to the beamline alive before experiments. Samples were measured on beamline 15U at the Shanghai Synchrotron Radiation Facility (Shanghai, China) with an electron beam energy of 3.5 GeV. The continuous synchrotron X-rays were monochromated using two flat Si(111) crystals. A monochromatic X-ray beam with photon energy of 16.3 keV was used to excite the samples. The focused X-ray beam was adjusted with horizontal slits to a beam size of 6.68 μm $\times$ 2 μm. The excitation energy was adjusted to 16.3 keV. The element distribution was continuously scanned with a step of 0.1 μm in both the *x* and *y* directions. Each spot was irradiated for 0.5 s. A seven-element, 50 mm^2 Si(Li) detector array (Vortex USA) was used to collect the fluorescence signal. The two-dimensional maps of elements were analyzed using the software *Matlab* 7.12.0. Sample hotspots were identified based on synchrotron radiation μ-XRF mapping in areas with higher element concentrations.

2.5. XANES spectroscopy

XANES is commonly applied to bulk samples in transmission mode. However, fluorescence mode is more appropriate for diluted samples. XANES experiments were carried out at the same beamline in fluorescence mode. The Pb L_3-edge was set to 13035 eV using the first maximum of the first derivative of the Pb foil spectrum. XANES spectra were measured with 0.5 eV equidistant energy steps in the edge region from 12985 eV to 13155 eV. Powder references were analyzed in transmission mode, liquid references were placed in liquid

sample holders, and all plant samples were stuck on adhesive tape without sulfur. All powder and plant samples were measured in fluorescence mode, and liquid samples were measured in transmission mode using a 32-element Ge solid-state detector array (Vortex USA). Measurements of plants samples were repeated twice to ensure reproducibility. All sample measurements were performed under ambient air pressure and room temperature conditions. The data were normalized using a second-order spline for pre- and post-edge regions and analyzed using the software *ATHENA* 0.8.061 (Ravel & Newville, 2005).

3. Results and discussion

3.1. Organic ligands inhibit Pb absorption into *Arabidopsis*

Pb complexes with organic ligands can change the uptake capability of plant roots. Some Pb-organic complexes increase Pb uptake, while others reduce it (Farrell *et al.*, 2010; Ho, 2005; Orsetti *et al.*, 2013). However, most researchers have used $Pb(NO_3)_2$ in the cultivation of plants in Pb exposure experiments. To examine the effects of organic matter and Pb-organic complexes on the Pb uptake and growth of plants, $Pb(NO_3)_2$ and $Pb(CH_3COO)_2$ were used to treat *A. thaliana* plants.

The Pb accumulation in 30 day-old *A. thaliana* seedlings increased with increased concentrations of inorganic Pb [$Pb(NO_3)_2$] and organic Pb [$Pb(CH_3COO)_2$] in the nutrient solution, as shown in Fig. 1. However, the average concentrations of Pb in *Arabidopsis* grown under $Pb(NO_3)_2$ were higher than in those cultivated under $Pb(CH_3COO)_2$. The maximum average Pb concentrations in *Arabidopsis* were 2717 and 2348 p.p.m. for inorganic and organic Pb, respectively. These results revealed that *Arabidopsis* absorbed more Pb from $Pb(NO_3)_2$ than $Pb(CH_3COO)_2$.

3.2. Effects of inorganic and organic Pb on roots

Roots play a dominant role in the accumulation of toxic elements by plants as they have direct contact with elements in the soil and affect uptake processes, particularly uptake from the soil and translocation to shoots through the stem. Root length and lateral root number are the most important parameters for heavy metal toxicity to plants. As shown in Fig. 2(*a*), when exposed to 0–5 p.p.m. $Pb(NO_3)_2$, *Arabidopsis* showed a root length decrease from 1.88 to 1.60 cm, and then an increase under exposure concentrations of 5 to 20 p.p.m. from 1.60 to 1.91 cm. After reaching a peak value at an exposure concentration of 20 p.p.m., root length dropped from 1.911 cm to 1.13 cm (exposure concentration 200 p.p.m.). The organic Pb group showed a similar pattern: a decrease
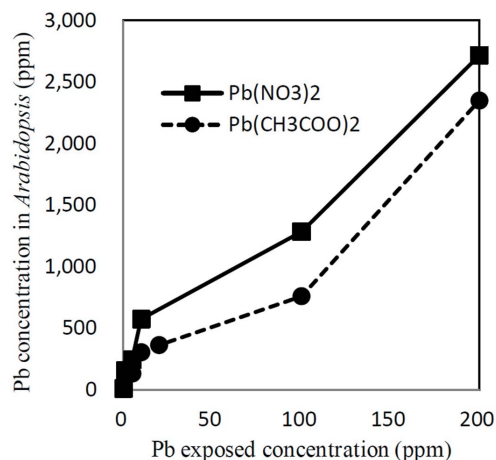

Figure 1
Pb concentration in 11 day-old *Arabidopsis thaliana* plants exposed to inorganic and organic Pb.

from 1.88 cm to 1.38 cm and then an increase from 1.37 cm to 1.78 cm, followed by another decrease from 1.78 cm to 0.24 cm. The inhibitory effect reached a maximum at 200 p.p.m. for both groups. The inhibition of primary root length in *Arabidopsis* by $Pb(CH_3COO)_2$ was 2.2 times greater than that by $Pb(NO_3)_2$ at the same exposure concentration (200 p.p.m.).

Lateral roots determine the final shape of the root system and affect the plant's ability to uptake water and nutrients. The root system of *A. thaliana* consists of an embryo-derived primary root from which secondary lateral roots are continuously produced. Auxin plays an essential role in many aspects of plant development. Its dynamic and differential distribution within the plant is regulated by a variety of environmental cues including heavy metal stimuli. The average number of lateral roots was similar between the organic and inorganic Pb groups (Fig. 2*b*). Many more lateral roots were produced by *Arabidopsis* between 10 and 50 p.p.m. in the $Pb(NO_3)_2$ group, while the organic ligand inhibited lateral root growth at all Pb concentrations.
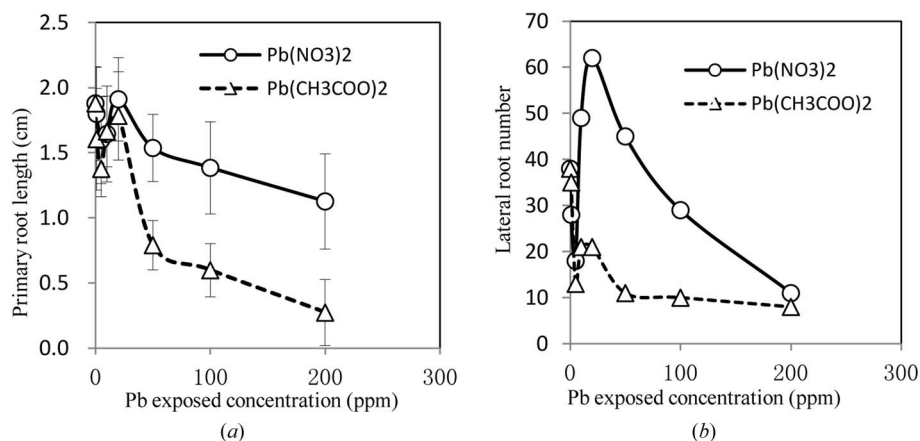

Figure 2
Root characteristics [(*a*) primary root length; (*b*) lateral root number] of *Arabidopsis* exposed to organic and inorganic Pb.

It was reported that $Pb(CH_3COO)_2$ was more toxic to animals than $Pb(NO_3)_2$ (Nageshwar *et al.*, 2012) but little is known about the effects of these Pb complexes on plants. This study revealed that the toxicity of $Pb(CH_3COO)_2$ and its damage to plants were greater than $Pb(NO_3)_2$. A previous study showed that Pb^{2+} could decrease the primary root length and increase the lateral root density (Wang *et al.*, 2015), which is similar to our results for the inorganic Pb group. However, with the organic ligand, the decrease in primary root length was much greater and, moreover, it inhibited the stimulation of lateral root density. Thus, the heavy metal concentration and effects of organic ligands should be considered when discussing the inhibition or promotion of root growth by Pb.

3.3. Pb distribution in roots exposed in inorganic and organic Pb

Iron plaque formation on root surfaces is widely observed in wetland plants. It is generally accepted that Fe plaques are formed where oxygen released from the roots reacts with reduced soluble Fe^{2+} to form a smooth, regular reddish precipitate or irregular plaque coating on the root surface (Amils *et al.*, 2007). Fe plaques can sequester metals on root surfaces and therefore influence metal uptake and tolerance by wetland plants (Blute *et al.*, 2004).

Because of the detection limits of μ-XAS and mapping time limitation of μ-XRF, 4 day-old *Arabidopsis* shoots exposed to 200 p.p.m. inorganic and organic Pb were chosen separately for element distribution analysis using μ-XRF. Pb was accumulated mainly in the root and only a small proportion of the total Pb taken up was transported to the shoot (Fig. 3), which was similar to previous research (Phang *et al.*, 2011). The formation of point-like Fe plaques was observed in the root while Pb was distributed over almost the whole root.

As shown in Fig. 4, *Arabidopsis* grew faster in $Pb(CH_3COO)_2$ than when exposed to $Pb(NO_3)_2$ at an early stage (4 days-old). The Fe and Pb distribution characteristics of *Arabidopsis* roots exposed to $Pb(CH_3COO)_2$ are also shown in Fig. 4. Pb was deposited mainly and intensively on the surface of small root hairs where Fe plaques formed. As shown in the previous section, the organic ligand inhibited Pb absorption more than the inorganic ligand. The relative Pb content of roots exposed to $Pb(CH_3COO)_2$ was much greater than those exposed to $Pb(NO_3)_2$; this can be explained by the organic ligand helping Fe plaques to adsorb Pb, which protects the plant from Pb toxicity.

It was reported that Se adsorbed in iron plaques could be desorbed by low-molecular-weight organic acids (Zhou *et al.*,
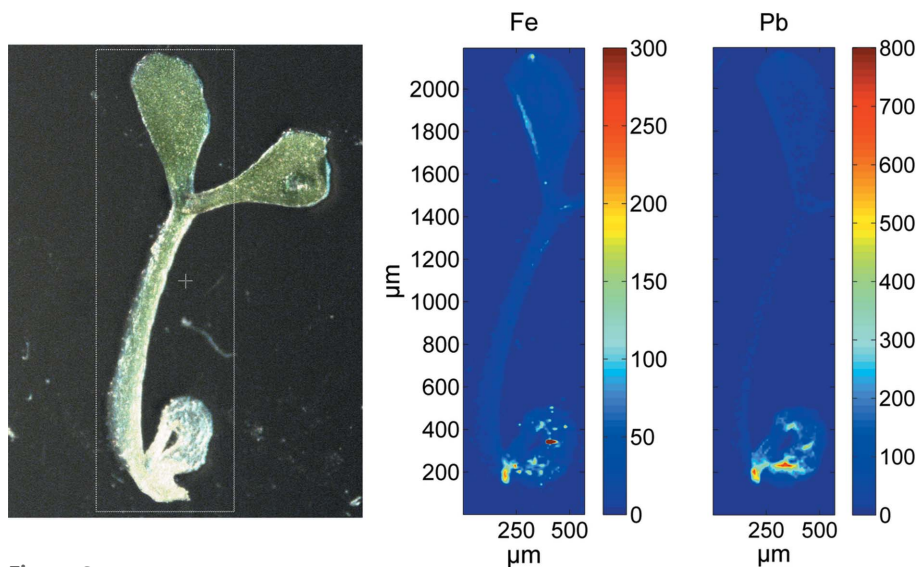
Figure 3
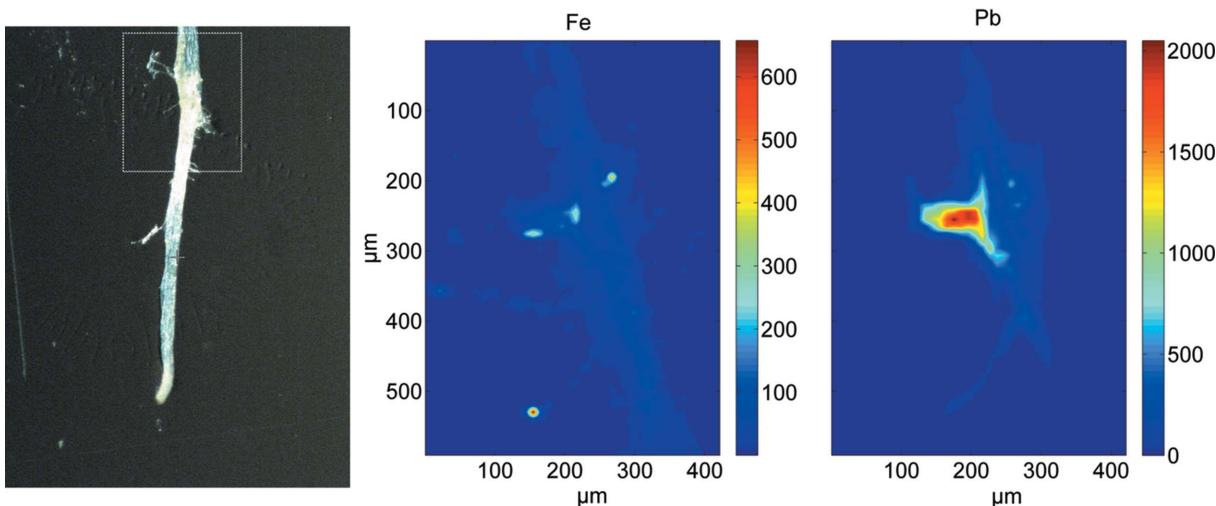Fe and Pb distribution in 4 day-old shoots exposed to 200 p.p.m. $Pb(NO_3)_2$.

Figure 4
Fe and Pb distribution in 4 day-old shoots exposed to 200 p.p.m. $Pb(CH_3COO)_2$.

2007), which explains why Fe plaques in the rhizosphere prevented roots exposed to $Pb(CH_3COO)_2$ from absorbing Pb.

3.4. Pb speciation in *Arabidopsis* exposed in inorganic and organic Pb

Pb speciation in plants plays a key role in the transformation, transport and function of Pb within the organism. Organic ligands not only affect absorption but also change the antioxidant response and detoxification mechanisms, which comes from the Pb species change. Difficulties in identifying ligands and Pb-ligands in plant fluids are inherent to their ability to form metal complexes. Errors in ligand quantification always occur during sample extraction, treatment and analytical determination, because of either the complete dissociation of the existing metal complexes or the quantitative formation of metal complexes. XANES is a useful approach for identifying metal complexes in plant tissues that relies on the identification of the chemical environment surrounding the metal, which allows the direct detection of *in situ* metal speciation in plants without any preliminary extraction or preparation.

The XANES spectra analysis was performed by pre-edge and post-edge background subtraction followed by normalization using *ATHENA*. First, 13035 eV was set as E_0, and then the energy range was set to −20 to 70 eV, which contains the 'white line' and the second obvious oscillation of the spectrum line. Each spectrum gave a different white line position and first derivative characteristics, especially for $C_{32}H_{66}PbS_2$, which represents a structure similar to Pb-binding proteins. The Pb L_3 spectra for plants in both the organic and inorganic Pb groups appeared similar to those of small organic acid-Pb and FA-Pb (Fig. 5).

Principal component analysis (PCA) assumes that the absorbance of references (a set of 14 XANES spectra here) can be mathematically represented by a linear combination of independent components known as factors. The maximum absolute value of the residual between the measured XANES spectrum and the reconstructed data was used for the components chosen (Luo *et al.*, 2016). When the first two principal components were chosen, the maximum absolute value of the residual between the measured XANES spectrum and the reconstructed data was 0.32. The maximum absolute value of the residual decreased sharply to 0.06 when the top three components were chosen, but choosing the first four components did not improve the maximum absolute value of the residual (0.04). Thus, the top three components were chosen here for linear combination fitting (LCF) analysis. After reconstruction of each of the 14 references, the following references were used for LCF: $Pb(CH_3COO)_2$, $Pb_5(PO_4)_3Cl$, $Pb(C_{17}H_{35}COO)_2$, $C_{32}H_{66}PbS_2$, Pb-citric acid and Pb-FA. These results were reasonable considering reports that small organic acid-Pb, $Pb_5(PO_4)_3Cl$, Pb-COO, Pb-O-CH_3 and Pb-S are the most important Pb species in plants (Mah & Jalilehvand, 2012; Kopittke *et al.*, 2008; Lamelas *et al.*, 2009;

Table 1
Linear combination fitting results for Pb speciation in two groups of *Arabidopsis* exposed to inorganic and organic Pb.

Arabidopsis exposed group	Standard	Weight	R-factor	χ^2	Reduced χ^2
$Pb(NO_3)_2$	Citric acid-Pb	0.779 (0.056)	0.0017989	0.03794	0.0002448
	FA-Pb	0.142 (0.081)			
	$C_{32}H_{66}PbS_2$	0.079 (0.020)			
$Pb(CH_3COO)_2$	Citric acid-Pb	0.501 (0.057)	0.0012756	0.02764	0.0001760
	FA-Pb	0.396 (0.072)			
	$C_{32}H_{66}PbS_2$	0.104 (0.017)			

Alvarez-Fernandez *et al.*, 2014). The Pb L_3-edge absorption spectral lines of the samples, fitting results and standard references are shown in Fig. 5. LCF using citric acid-Pb, FA-Pb and $C_{32}H_{66}PbS_2$ fit well to the results for the two Pb species in *Arabidopsis* exposed to Pb (see Table 1).

Possible ligand candidates are a range of small molecules, including organic acids–carboxylates, such as citrate and malate, amino acids, including nicotianamine, histidine, cysteine and high-affinity Fe(III)-chelating compounds derived from nicotianamine called phytosiderophores, such as mugineic and deoxy mugineic acids, as well as peptides and proteins (*e.g.* metallothioneins) (Alvarez-Fernandez *et al.*, 2014).

The results showed that Pb-citric acid was the main species in *Arabidopsis* exposed to both inorganic and organic Pb. Because *Arabidopsis* plants exposed to $Pb(NO_3)_2$ absorbed more Pb than those exposed to $Pb(CH_3COO)_2$, but less Pb was deposited in the root in the $Pb(NO_3)_2$ group, it can be inferred that long-distance transportation may be more active at higher Pb concentrations without organic ligands because the bioavailability of heavy metals is related to their solubility and mobility. It was reported that Pb solubilization was
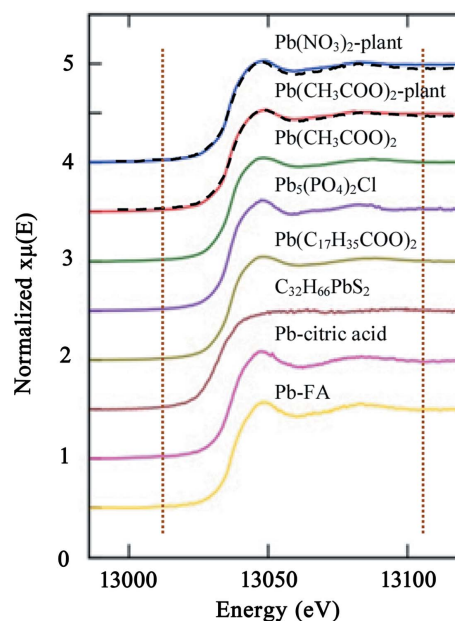

Figure 5
Pb L_3-edge absorption spectral lines of samples and standard references, and linear combination fitting results (linear combination fitting results are indicated with dashed lines; the fitting range was −20 to 70 eV).

affected by local competition between Pb^{2+} and $H^+(Ca^{2+})$ for solid phase adsorption, which leads to the production of protons in the rhizosphere and the generation of small molecular organic acids (Fest *et al.*, 2008) and dissolved organic matter (Kim, Lim *et al.*, 2010; Kim, Owens *et al.*, 2010). Carboxylates are usually found within the μM–mM range in plant fluids, whereas nicotianamine, deoxy mugineic acids, histidine and other molecules are generally in the μM range (Alvarez-Fernandez *et al.*, 2014). It was inferred that $Pb(CH_3COO)_2$ maintained the protonation process, which improved availability compared with $Pb(NO_3)_2$. Here, the results provide indirect evidence to suggest that long-distance organic ligand-assisted transport of metals is significantly inhibited by organic ligands at relatively high Pb concentrations (200 p.p.m.) to protect plants from toxicity and oxidative stress.

4. Conclusions

Plants absorbed more Pb from $Pb(NO_3)_2$ than $Pb(CH_3COO)_2$ at the same concentration [*e.g.* the absolute content in *Arabidopsis* grown in 100 p.p.m. $Pb(NO_3)_2$ was 369 p.p.m. higher than in plants grown in 100 p.p.m. $Pb(CH_3COO)_2$]. However, $Pb(CH_3COO)_2$ was more physiologically toxic than $Pb(NO_3)_2$ to *A. thaliana*. Inhibition of primary root length by $Pb(CH_3COO)_2$ was much greater than that by $Pb(NO_3)_2$. $Pb(NO_3)_2$ stimulated lateral root generation while $Pb(CH_3COO)_2$ inhibited lateral root density compared with the control group. $Pb(CH_3COO)_2$ was more likely to be accumulated on the root surface, which resulted in a relative local Pb concentration 2.5 times higher than that under $Pb(NO_3)_2$. LCF results showed that more Pb-citrate was present in *Arabidopsis* exposed to $Pb(CH_3COO)_2$, which provides indirect evidence that organic ligand-assisted transport of metals is significantly inhibited by organic ligands to protect plants from toxicity and oxidative stress.

References

Alvarez-Fernandez, A., Diaz-Benito, P., Abadia, A., Lopez-Millan, A.-F. & Abadia, J. (2014). *Front. Plant Sci.* **5**, 1–20.

Amils, R., de la Fuente, V., Rodríguez, N., Zuluaga, J., Menéndez, N. & Tornero, J. (2007). *Plant Physiol. Biochem.* **45**, 335–340.

Arshad, M., Silvestre, J., Pinelli, E., Kallerhoff, J., Kaemmerer, M., Tarigo, A., Shahid, M., Guiresse, M., Pradere, P. & Dumat, C. (2008). *Chemosphere*, **71**, 2187–2192.

Babich, H. & Stotzky, G. (1979). *Appl. Environ. Microbiol.* **38**, 506–513.

Bech, J., Reverter, F., Tume, P., Sanchez, P., Longan, L., Bech, J. & Oliver, T. (2011). *J. Geochem. Explor.* **109**, 26–37.

Blute, N. K., Brabander, D. J., Hemond, H. F., Sutton, S. R., Newville, M. G. & Rivers, M. L. (2004). *Environ. Sci. Technol.* **38**, 6074–6077.

Evangelou, M. W. H., Ebel, M. & Schaeffer, A. (2007). *Chemosphere*, **68**, 989–1003.

Farrell, M., Perkins, W. T., Hobbs, P. J., Griffith, G. W. & Jones, D. L. (2010). *Environ. Pollut.* **158**, 55–64.

Fest, E. P. M. J., Temminghoff, E. J. M., Comans, R. N. J. & van Riemsdijk, W. H. (2008). *Geoderma*, **146**, 66–74.

Fleming, M., Tai, Y., Zhuang, P. & McBride, M. B. (2013). *Environ. Pollut.* **177**, 90–97.

Giaccio, L., Cicchella, D., De Vivo, B., Lombardi, G. & De Rosa, M. (2012). *J. Geochem. Explor.* **112**, 218–225.

Ho, Y. S. (2005). *Bioresour. Technol.* **96**, 1292–1296.

Kim, K.-R., Owens, G., Naidu, R. & Kwon, S. (2010). *Geoderma*, **155**, 86–92.

Kim, S., Lim, H. & Lee, I. (2010). *J. Biosci. Bioeng.* **109**, 47–50.

Kopittke, P. M., Asher, C. J., Blamey, F. P. C., Auchterlonie, G. J., Guo, Y. N. & Menzies, N. W. (2008). *Environ. Sci. Technol.* **42**, 4595–4599.

Lamelas, C., Pinheiro, J. P. & Slaveykova, V. I. (2009). *Environ. Sci. Technol.* **43**, 730–735.

Liu, J. & Luo, L. Q. (2015). *Rock Mineral Anal.* **34**, 269–277.

Luo, L., Shen, Y., Liu, J. & Zeng, Y. (2016). *At. Spectrosc.* **122**, 40–45.

Mah, V. & Jalilehvand, F. (2012). *Inorg. Chem.* **51**, 6285–6298.

Margui, E., Salvadó, V., Queralt, I. & Hidalgo, M. (2004). *Anal. Chim. Acta*, **524**, 151–159.

Nageshwar, W., Gaherwal, S. & Prakash, M. M. (2012). *J. Environ. Res. Dev.* **6**, 743–747.

Orsetti, S., Marco-Brown, J. L., Andrade, E. M. & Molina, F. V. (2013). *Environ. Sci. Technol.* **47**, 8325–8333.

Phang, I. C., Leung, D. W. M., Taylor, H. H. & Burritt, D. J. (2011). *Plant Growth Regul.* **64**, 17–25.

Pourrut, B., Shahid, M., Dumat, C., Winterton, P. & Pinelli, E. (2011). *Rev. Environ. Contam. Toxicol.* **213**, 113–136.

Ravel, B. & Newville, M. (2005). *J. Synchrotron Rad.* **12**, 537–541.

Schreck, E., Foucault, Y., Sarret, G., Sobanska, S., Cécillon, L., Castrec-Rouelle, M., Uzu, G. & Dumat, C. (2012). *Sci. Total Environ.* **427–428**, 253–262.

Shahid, M., Dumat, C., Silvestre, J. & Pinelli, E. (2012). *Biol. Fertil. Soils*, **48**, 689–697.

Shahid, M., Ferrand, E., Schreck, E. & Dumat, C. (2013). *Rev. Environ. Contamin. Toxicol.* **221**, 107–127.

Shahid, M., Pinelli, E., Pourrut, B. & Dumat, C. (2014). *J. Geochem. Explor.* **144**B, 282–289.

Shahid, M., Pinelli, E., Pourrut, B., Silvestre, J. & Dumat, C. (2011). *Ecotoxicol. Environ. Saf.* **74**, 78–84.

Templeton, A. S., Trainor, T. P., Traina, S. J., Spormann, A. M. & Brown, G. E. (2001). *Proc. Natl Acad. Sci. USA*, **98**, 11897–11902.

Wahsha, M., Bini, C., Fontana, S., Wahsha, A. & Zilioli, D. (2012). *J. Geochem. Explor.* **113**, 112–117.

Wang, R., Wang, J., Zhao, L., Yang, S. & Song, Y. (2015). *Biometals*, **28**, 123–132.

Wang, T. J., Pan, J., Liu, X. I. (2016). *Rock Mineral Anal.* **35**, 425–432.

Zhou, X. B., Shi, W. M. & Zhang, L. H. (2007). *Plant Soil*, **290**, 17–28.